Viscoelasticity of F-Actin Measured with Magnetic Microparticles

Ken S. Zaner* and Peter A. Valberg‡

*Hematology-Oncology Section, Boston City Hospital and Boston University School of Medicine, Boston, Massachusetts 02118; and ‡Respiratory Biology Program, Department of Environmental Science and Physiology, Harvard School of Public Health, Boston, Massachusetts 02115

Abstract. Dispersed submicroscopic magnetic particles were used to probe viscoelasticity for cytoplasm and purified components of cytoplasm. An externally applied magnetic field exerted force on particles in cells, in filamentous actin (F-actin) solutions, or in F-actin gels formed by the addition of the actin gelation factor, actin-binding protein (ABP). The particle response to magnetic torque can be related to the viscoelastic properties of the fluids. We compared data obtained on F-actin by the magnetic particle method with data obtained on F-actin by means of a sliding plane viscoelastometer. F-actin solutions had a significant elasticity, which increased by 20-fold when gels were formed by ABP addition. Both methods gave consistent results, but the dispersed magnetic particles indicated quantitatively greater rigidity than the viscoelastometer (two and six times greater for F-actin solutions and for F-actin plus ABP gels, respectively). These differences may be due to the fact that, compared with traditional microrheometers, dispersed particle measurements are less affected by long-range heterogeneity or domain-like structure. The magnetometric method was used to examine the mechanical properties of cytoplasm within intact macrophages; the application of the same magnetometric technique to both cells and well-defined, purified protein systems is a first step toward interpreting the results obtained for living cells in molecular terms. The magnetic particle probe system is an effective nonoptical technique for determining the motile and mechanical properties of cells in vitro and in vivo.

CYTOPLASM has the capacity to both generate motion and resist deformation. However, surprisingly little is known about the mechanical factors involved in cell spreading, locomotion, phagocytosis, organelle movement, and division. Cytoplasmic motion in macrophages has been tracked using incorporated magnetic particles, which respond both to endogenous cytoplasmic forces and to externally applied magnetic fields (Valberg and Albertini, 1985). These particles can convey information magnetometrically on the rate of cytoplasmic motion, on the non-Newtonian viscosity of cytoplasm, and on the elasticity of cytoplasm (Valberg and Albertini, 1985; Nemoto et al., 1989). Recent attention has been focused on the relation of intracellular motility to the viscoelastic properties of purified F-actin and microtubule suspensions (Buxbaum et al., 1987).

The properties of a number of the structural and force-generating proteins of the cortical cytoplasm have been recently reviewed (Elson, 1988; Stossel, 1988). One important constituent of the cortical cytoplasm that is ubiquitously present in motile cells is the microfilament system, which consists of filamentous actin (F-actin). F-actin is a linear polymer that can be cross-linked by a 540-kD molecular mass protein known as actin binding protein (ABP).[1] ABP, which is related in structure to a smooth muscle protein called filamen, gels F-actin by binding filaments together into orthogonally branched structures (Hartwig and Shevlin, 1986). A complete understanding of how F-actin structure contributes to its mechanical properties is presently unavailable. However, the mechanical properties of F-actin at different filament lengths and protein concentrations has been measured by a number of rheologic techniques and found generally to conform to a few simple principles of polymer physics. For example, the modulus of rigidity of actin solutions is approximately that expected for a system of entangled, stiff rods (Zaner and Hartwig, 1988). However, other data suggest that there are filament–filament interactions that must be taken into account in addition to the topological effect of entanglements (Sato et al., 1985; Buxbaum et al., 1987; Cortese and Frieden, 1988).

To better understand in molecular terms the rheologic information obtained from intact cells by the magnetic particle method (Valberg and Feldman, 1987; Valberg and Butler, 1987), we used magnetometry to measure the mechanical properties of F-actin solutions and gels formed by cross-linking F-actin with ABP. A particular advantage of the magnetic particle approach is that, in contrast to conventional rheologic methods, which are "bulk" measurements, the magnetic particle method probes rheology at the "microscopic" level.

1. *Abbreviations used in this paper*: ABP, actin-binding protein; RMF, remanent magnetic field.

The central idea was to magnetically monitor the movement of particles enmeshed in F-actin. Proteins and other cell components are not ferromagnetic, but tiny ferromagnetic crystals can be introduced as probe particles. Such particles can be magnetically aligned by application of a strong magnetic field, and particle rotation can be followed magnetometrically by measuring changes in the particles' remanent magnetic field (RMF). The magnitude of the RMF and its time course after magnetization depend, respectively, on the quantity of magnetic material present and on the degree of particle motion. A torque can be applied to magnetic particles by external fields, and the rate of particle rotation in response to this torque measures the apparent viscoelasticity of the medium surrounding the particles (Valberg and Butler, 1987).

Materials and Methods

F-Actin Preparation

Actin was purified using the method of Spudich and Watt (1971) from an acetone powder of rabbit skeletal muscle. Purified actin was stored in the depolymerized form in buffer A (2 mM Tris, 0.2 mM $CaCl_2$, 0.5 mM ATP, 0.5 mM Eagle's basal medium, pH 7.5) at 4°C and was used within 4 d of purification. ABP was purified from rabbit lung macrophages by the method of Hartwig and Stossel (1981). G-actin was prepared in concentrations ranging from 2 to 8 mg/ml. G-actin, with or without ABP, was allowed to polymerize for 2 h in the presence of magnetic iron oxide particles (γ-Fe_2O_3) at a concentration of 50 μg/ml. When ABP was added, the molar ratio of ABP to actin monomer was 1:200. After protein mixture preparation and magnetic particle dispersal, we adjusted the salt concentration to 2 mM $MgCl_2$ and 0.1 mM KCl.

Magnetic microparticles were generated in aerosol form by controlled combustion of iron pentacarbonyl vapors (Valberg and Brain, 1979). About 3 mg γ-Fe_2O_3 was collected on each of 10 filters for later dispersion into test fluids. Using an electrostatic point-to-plane precipitator, we collected particles onto carbon-coated copper grids and shadowed them for examination by electron microscopy. Particles were suspended in a series of Newtonian viscosity standards (dimethylpolysiloxane fluids); both relaxation and forced rotation were measured in viscosity standards so that the magnetic torque acting on the particles could be calibrated.

Viscoelastometer Measurements

The viscoelastometer uses a 0.001-inch-thick mica plate moving at a slow rate through a cuvette containing a small sample volume. The mica plate is mounted on the end of a pendulum that is suspended from a knife edge; motion is generated by sinusoidally tilting the table supporting the viscoelastometer. The component of gravitational force acting to keep the pendulum hanging vertically causes the mica plate to generate an oscillatory shear stress in the sample volume. The resulting movement of the pendulum is electronically sensed and is used to calculate the strain (Zaner et al., 1981).

Compliance and viscosity were measured by viscoelastometer on F-actin and F-actin plus ABP samples. Samples with and without embedded magnetic microparticles were compared. The viscoelastometer measurements were interpreted in terms of compliance, modulus of rigidity, and viscosity, as has been previously described (Zaner and Stossel, 1983; Zaner, 1986). No significant differences in rheological properties were found between the F-actin gel with and without iron oxide particles.

Magnetometry

After viscous fluids or F-actin gels had been prepared with dispersed magnetic microparticles, the following observations were made. The magnetic directions of particles were aligned (using a pulsed magnetic field of 93 millitesla [930 gauss]) so that the particles produced a weak magnetic field, the RMF. The RMF magnitude was typically 3 nanotesla (30 microgauss) and was measured in a magnetically shielded apparatus with four fluxgate detectors (Valberg and Butler, 1987). The magnitude of the initial RMF is proportional to the quantity of magnetic material. The magnetization of each particle is permanent, but any rotation of the fluid-suspended particles reorients their magnetization directions. The fluxgate detectors are sensitive to the vector component of the RMF that is parallel to the initial direction of magnetization, and the result of any particle reorientation is that the net RMF sensed at the detector decreases.

An RMF decrease for particles in test solutions can result either from random, independent motions of each particle, driven by thermal energy (called relaxation), or from the action of an applied magnetic field, which rotates particles in unison (called twisting; note Eq. 2 below). The direction of the twisting field was perpendicular to the direction of particle initial magnetization, and the magnetic torque created acted to rotate particles into alignment with the direction of this applied field. The applied magnetic field is homogeneous and exerts no translational force on the magnetic particles, only a torsional force. Monitoring the RMF decrease from magnetic iron oxide particles can be used to quantify particle diffusive motion and particle rotation rate in response to a known torque. These particle motions are related to the viscoelasticity of the medium trapping the particles.

Both particle relaxation and particle twist were measured in viscosity standards so that the magnetic torque acting on the particles could be calibrated. For magnetic particles, the torque is proportional to the strength of the twisting field, but rotation of the particles is opposed by the viscosity of the suspending fluid. When the twisting field is first applied, it lies perpendicular to the particle magnetic moments, and the magnitude of the torque is largest. As particles begin to rotate toward the applied field, torque falls off, reaching zero when particle magnetic moments and twisting field are parallel. Hence, the maximum particle rotation that can result from torque application is one quarter of a turn or 90°. The RMF decay curve generated for particles in viscous standards provides a means of calculating the stress that particles are applying to their environment as a function of particle magnetic orientation relative to the twisting field.

For the F-actin gels, the magnitude of the applied twisting field ranged from 0 to 30 gauss; this magnetic field is too small to change the intrinsic magnetization of individual particles imparted by the highfield (930 gauss) pulse. The sample temperature was maintained at 25°C, and the RMF from particles enmeshed in the F-actin gel was first recorded in the presence of zero applied field. The twisting field was then turned on and off for 1-min periods. The rate at which particles reoriented toward the twisting field and then recoiled was recorded over 5 min. The particle rotation is opposed by both viscous and elastic forces arising from the F-actin gel, and the RMF data were analyzed to provide an estimate of apparent viscosity and elasticity.

Lung Macrophages

Hamster lung macrophages were obtained by lung lavage from animals that had breathed magnetic iron oxide aerosol 24–48 h previously (Valberg and Albertini, 1985). Because the aerosol inhalation had delivered particles to the surfaces of lung alveoli, the harvested cells contained submicrometric magnetic iron oxide particles within phagosomes and phagolysosomes. During magnetometry measurements, macrophages were maintained at 37°C in culture medium, adhered to the bottom of glass vials, and oxygenated. The intracellular particles were magnetized, and both their spontaneous motion and their motion in response to external magnetic torque were recorded magnetometrically.

Results

Particle Incorporation

The appearance of the magnetic particles was crystalline, with individual units ~0.2 μm in diameter and with agglomerates in chains ~0.5 μm long (Fig. 1). Average particle physical diameter was 0.34 μm, and diameter distribution was lognormal with a geometric standard deviation of 1.25. Light microscopy showed the particles to be uniformly dispersed throughout the actin solutions; there was no indication of particle sedimentation over 2 d after gel formation even though the particle density was 4.6 g/cm^3. It can be estimated that particle entrapment was quite efficient. For example, at an actin concentration of 6 mg/ml, there is a total length of $\sim 2 \times 10^{10}$ cm of filaments/ml of gel; this results in an interfilament separation of <0.1 μm, which corre-

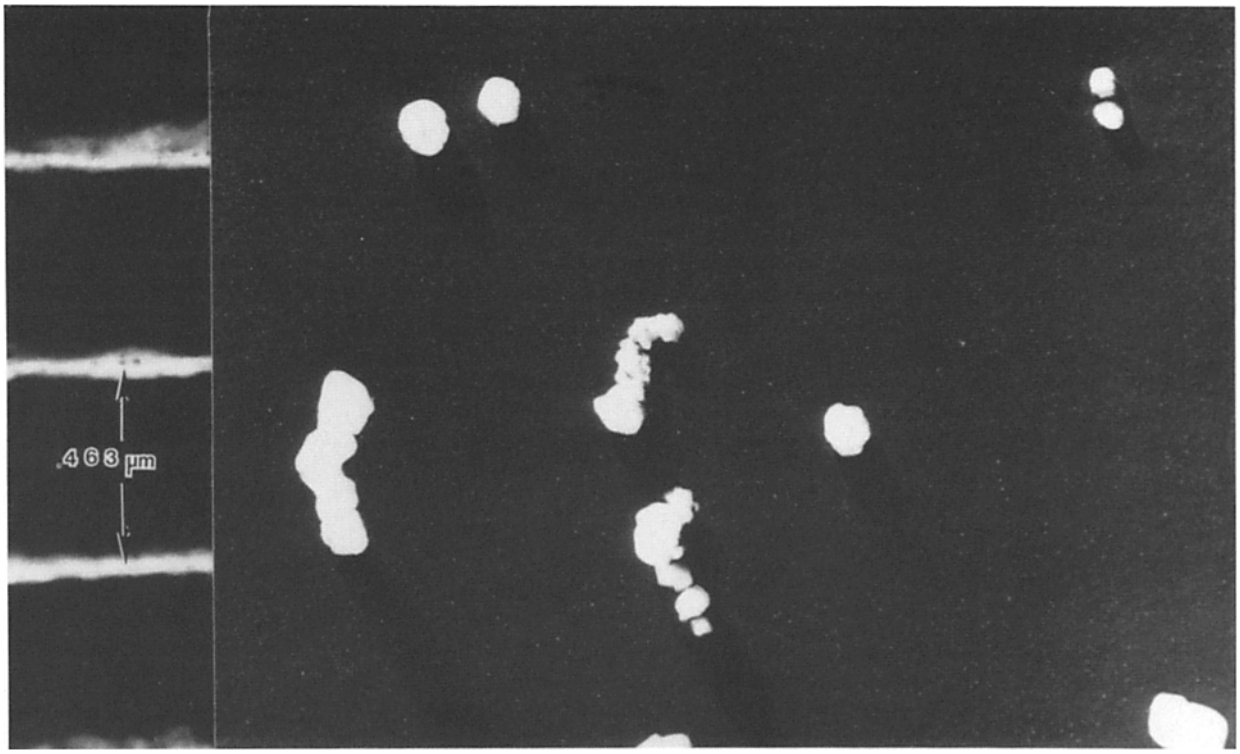

Figure 1. Electron micrograph of γ-Fe_2O_3 particles collected by electrostatic precipitation onto a carbon-coated grid from the aerosol. The grid was shadowed at 70° with gold-palladium and examined with an electron microscope (300; Philips Electronic Instruments, Inc., Mahwah, NJ). A calibration grating (54,860 lines per inch) was photographed at the same magnification to provide the length scale on the left (0.463 μm). The particles can be seen to consist of individual units ~0.2 μm in diameter with agglomerates in chains ~0.5 μm long.

sponds to a "pore size" of ~0.14 μm. Magnetic particle volume was ~0.001% of gel volume.

Magnetometric Studies of Viscosity Standards

Particle rotation in a 1,000-poise viscosity standard is shown in Fig. 2 *A*. The vertical axis gives the magnitude of the measured RMF; also shown are the correspondence of the vertical axis to the angle of particle rotation in degrees and to the stress being applied to the particles (dyne/cm²). Since this is an inertialess situation (Reynolds number of $\sim 10^{-4}$), magnetic torque (τ) and shear stress ($\eta\omega V$) are always in balance (η is viscosity, ω is rotation rate, and V is particle volume). The mathematical form of this curve has been analyzed previously (Valberg and Butler, 1987). If $B_r(t)$ is the RMF at time t and B_{r0} is the initial RMF, these are related to θ by

$$B_r(t) = B_{r0} \sin \theta, \quad (1)$$

where θ is the orientation of the magnetic axis of the particles relative to the twisting field. At $t = 0$, θ is 90° and then decreases towards zero. θ is related to time by (Valberg and Butler, 1987)

$$\ln [\tan (\theta/2)] = -t\, c/\eta, \quad (2)$$

where η is the viscosity of the dispersing fluid and c is the magnitude of the stress applied by the twisting field at $t = 0$. Particle rotation is independent of particle diameter because both the twisting force applied to the particles and the viscoelastic resistance offered by the fluid vary as the cube of particle diameter (see Valberg and Butler, 1987). Fig. 2 *B* shows a plot of ln tan (θ/2) vs. t, which should produce a straight line with slope c/η. Knowing that the viscosity of the fluid is 1,000 poise, we can calculate that c = 10.9 dyne/cm². The small deviations of plotted points from a straight line are likely due to the presence of a small fraction of particles whose geometry deviates quite significantly from spherical.

The relaxation due to Brownian motions of magnetic particles suspended in viscous fluid is given by (Nemoto, 1982)

$$B_r(t) = e^{-\lambda t}, \quad (3)$$

where $\lambda = 2kT/\pi\eta d^3$ (k is the Boltzmann constant, T is the absolute temperature, η is the fluid viscosity, and d is the particle diameter). From the relaxation curve in Fig. 2 *A*, we can estimate λ and calculate that average particle hydrodynamic diameter was 0.61 μm. Fig. 2 *C* illustrates the behavior of the RMF when the twisting field was turned on and off. The viscosity standards exhibited no recoil upon release of stress.

Magnetometric Studies of Actin Systems

The time course of the RMF for magnetic particles dispersed in solutions having F-actin concentrations of 11.1, 5.5, and 2.2 mg/ml is shown in Fig. 3. The upper curves are the decay of the RMF in the absence of a twisting field and, thus, represent Brownian movement of the particles. The decay rate increases as the concentration of F-actin decreases. Brownian movement of the magnetic particles is very evident at the lower F-actin concentrations, and, at 11.1 mg/ml, the

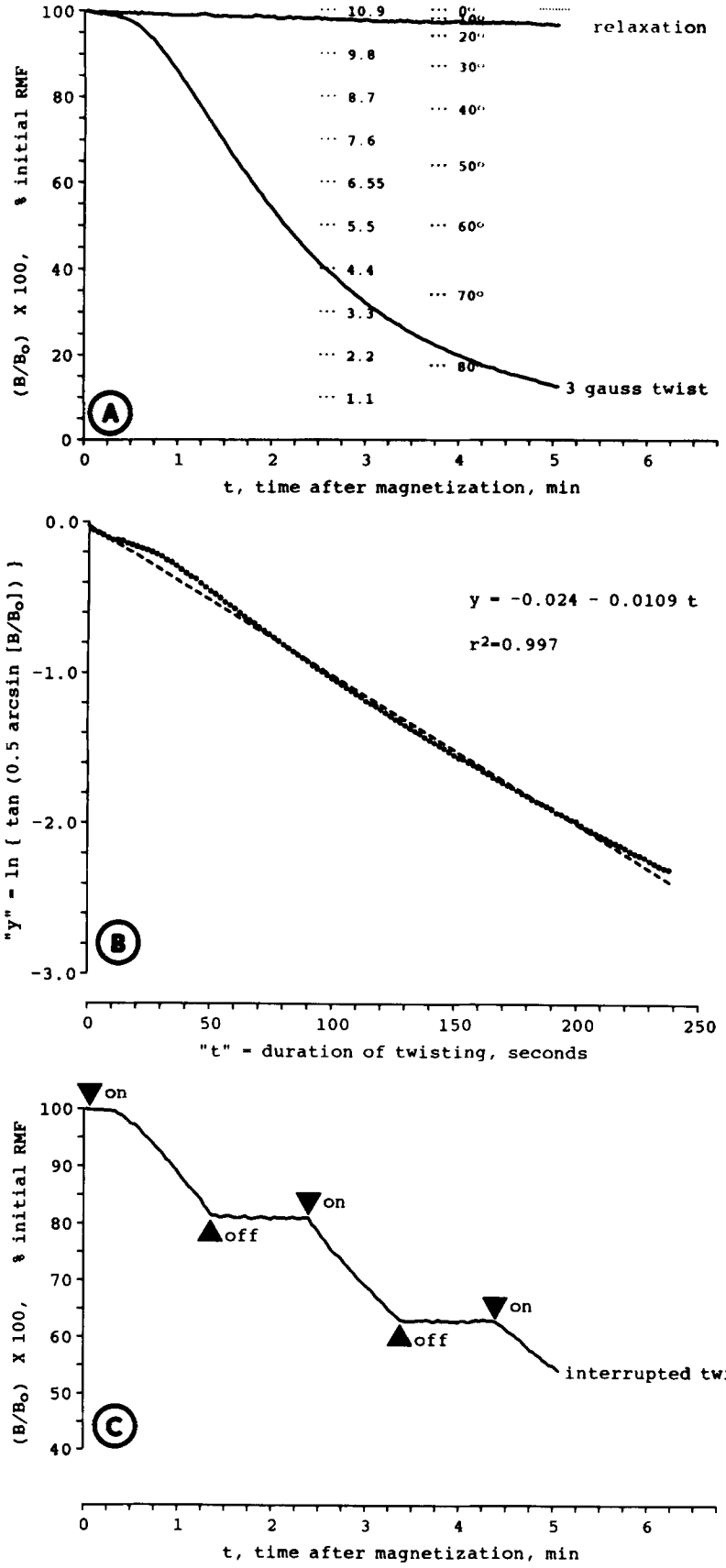

Figure 2. (*A*) RMF as a function of time for particles suspended in 1,000 poise dimethylpolysiloxane. The upper curve shows the decay of the RMF due to particle thermal motions, and the lower curve shows the decrease of the RMF as driven by a 3-gauss twisting field perpendicular to the original magnetization. (*B*) By fitting the data of RMF decay to the known fluid mechanics of particle rotation in a viscous fluid in response to an applied torque, we can see that the data fit the predictions of fluid mechanics and can calculate that the stress applied to the particles (torque per unit volume of particles) is 10.9 dyne/cm^2 when particle magnetization is perpendicular to the 3-gauss applied field. For larger or smaller fields, the stress applied would be correspondingly larger or smaller. (*C*) When the twisting field is turned on and off in 1-min intervals (*arrowheads*) particle rotation occurs only during the time the field is on. This result for the viscosity standards should be contrasted with subsequent figures showing the response of F-actin to on and off cycles of particle twist.

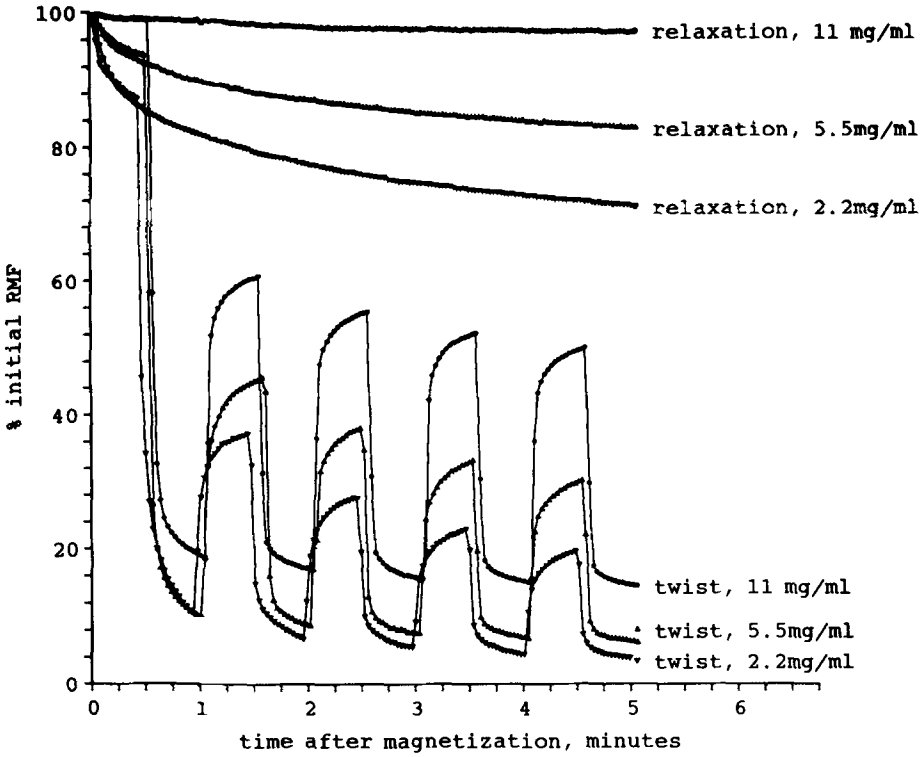

Figure 3. Upper curves depict relaxation of RMF in F-actin solutions of three different concentrations. Lower curves show the response of the embedded particles (in terms of the RMF) to 30-s on and off cycles of the twisting field (5 gauss).

decay rate is small, but definitely present. To examine the response of the system to an applied stress, a 5-gauss twisting field was applied to the sample in 30-s on and off cycles. The lower curves illustrate the results. It should be remembered that as the particles turn away from their original perpendicular orientation to the twisting field ($\theta = 90°$) the torque applied to the particles falls off as the function ($\sin \theta$). In contrast, as the particles turn away from their original equilibrium orientation in the gel, elastic restoring force increases with increasing rotation. Upon application of the twist field, the particles quickly rotated through an angle of ~78° for the 11.1 mg/ml F-actin sample and through ~84° for the 5.5 and 2.2 mg/ml samples. The initial rate at which the particles twisted was much more rapid than for the viscous standard depicted in Fig. 2 *A*. However, when the stress was released, the particle orientation recovered; the viscosity standards exhibited no recovery upon release of stress (Fig. 2 *C*). After completion of the first on and off cycle, the magnetization vector remained rotated by ~53, 63, and 69° for the 11.1, 5.5, and 2.2 mg/ml samples, respectively. Subsequent cycles of stress and release showed almost complete recovery of strain.

Fig. 4 *A* shows RMF curves for two different twisting field strengths applied in 1-min on and off cycles. When a 3-gauss twist is used, there is a 30° rotation after which there is almost complete recovery to the unperturbed decay level. The 6-gauss twist results in 48° rotation and less complete recovery. If the balance between elastic restoring force and magnetic torque is judged from the elastic recoil component in the curves for 3- and 6-gauss twisting fields, then the F-actin solution appears nearly linear. That is, the ratio of the torques being exerted at the point where the 1-min twist ends is nearly equal to the ratio of the angles through which the particles subsequently recoil. Fig. 4 *B* illustrates the result of twist application and release over a much longer time interval, (i.e., 5 min), particle rotation continues at a slow rate both in the twist and in the recoil phases. The flatness of the curve in the recoil phase reflects the competing effects of recoil (moving the curve upward) and relaxation (moving the curve downward). It suggests that the gel could be modeled by a Maxwell element in parallel with a spring.

The mechanical properties of F-actin over a range of strains is shown in Fig. 5 *A*. As the magnetic field–generated twisting force increased from 1.5 to 30 gauss, there was a progressive increase in the movement of the particles. In addition, the amount of strain recovery over 60 s after release of stress progressively decreased. However, a subsequent sequence of progressively increasing twisting pulses yielded nearly superimposable results. The data show that the viscoelastic behavior of this system was linear, or, in other words, the twisting of particles was not irreversibly disrupting the F-actin structure. This is further supported by the fact that a second relaxation measurement, made by remagnetizing the particles, was unchanged from the relaxation measured before the particle twisting protocol; thus, particle diffusion in the F-actin was not being enhanced by the twisting motions.

Upon application of stress, strain rate was initially rapid but then slowed. A time interval of 60 s was chosen because the majority of strain time dependence appeared to occur over this interval. The "secant modulus at 60 s," G_{60}, defined as the stress-to-strain ratio at 60 s, is shown in Table I; G_{60} is approximately equal to $G'(\omega)$, the dynamic storage modulus, at $\omega/2\pi = 2 \times 10^{-3}$ Hz. Fig. 5 *B* plots the relationship between stress and strain, as calculated from the data such as that in Fig. 5 *A*. The curve obtained has constant slope and extrapolates through the origin. The modulus falls only slightly over the range of twisting strengths examined, and the second set of measurements is close to the first. It is also

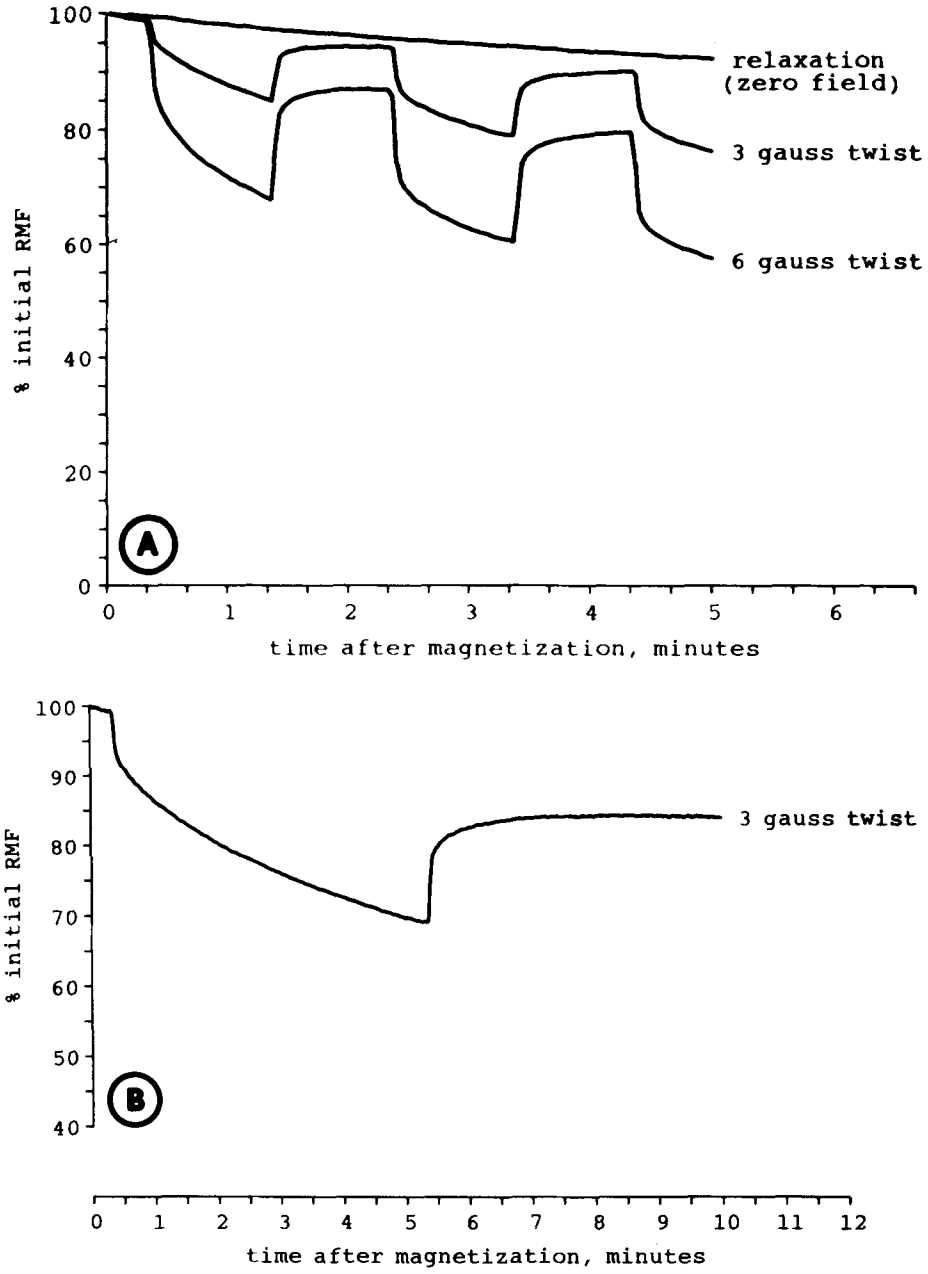

Figure 4. (*A*) The response of magnetic particles embedded in an F-actin solution (6.8 mg/ml) with an increase in the strength of the twisting field. After an initial 20 s without stress, the stress application and release (on and off) cycles are now 1 min. (*B*) If the length of the twist cycle is increased to 5 min as shown here, the RMF shows continuing decrement, indicating continuing particle rotation. Recoil also continues, at a decreasing rate, for 5 min after stress release.

of note that the rigidities obtained by this technique are within a factor of two of previously reported values using other, more conventional techniques (Zaner and Stossel, 1983).

The compliance, $J(t)$, of F-actin, calculated to be the strain-to-stress ratio, is shown Fig. 6 *A* as a function of duration of twist application. The compliance increases linearly with time at two different twisting values. Since the linear part of the compliance curve is proportional to t/η, the viscosity, η, can be calculated from this curve and is found to be 2,000 poise at a shear rate of 0.0025/s. This value is also in reasonable agreement with previously reported values (Zaner and Stossel, 1983).

The effect of ABP on F-actin, at a molar ratio of ABP to actin of 1:200, is shown in Fig. 7 *A*; the twisting field for both RMF curves was 30 gauss. Equivalent concentrations of F-actin (4 mg/ml) with and without ABP are shown in the upper and lower RMF curves, respectively. At a twisting field of 6 gauss, the particle movement was barely evident in the RMF curve of F-actin plus ABP on the scale of this graph, but it is plotted in Fig. 7 *B* at a tenfold increased vertical scale. The particle movement was <10°, and there was complete recovery of strain after release of stress. The overall downward direction of the time course reflects the greatly magnified effect of Brownian motion (relaxation) of the particles for the scale on this figure. The G_{60} is ~116 dyne/cm^2. At the larger stress (30 gauss; Fig. 7 *A*), there was a larger displacement of the particles, but again a complete recovery of strain. The calculated G_{60} is higher than at the lower strain and is ~153 dyne/cm^2. The compliance of the ABP plus actin mixture calculated from the data in Fig. 7 *A* is also shown in Fig. 6 *A*. It should be noted that the compliance is time independent over the course of the twist and, at the end of

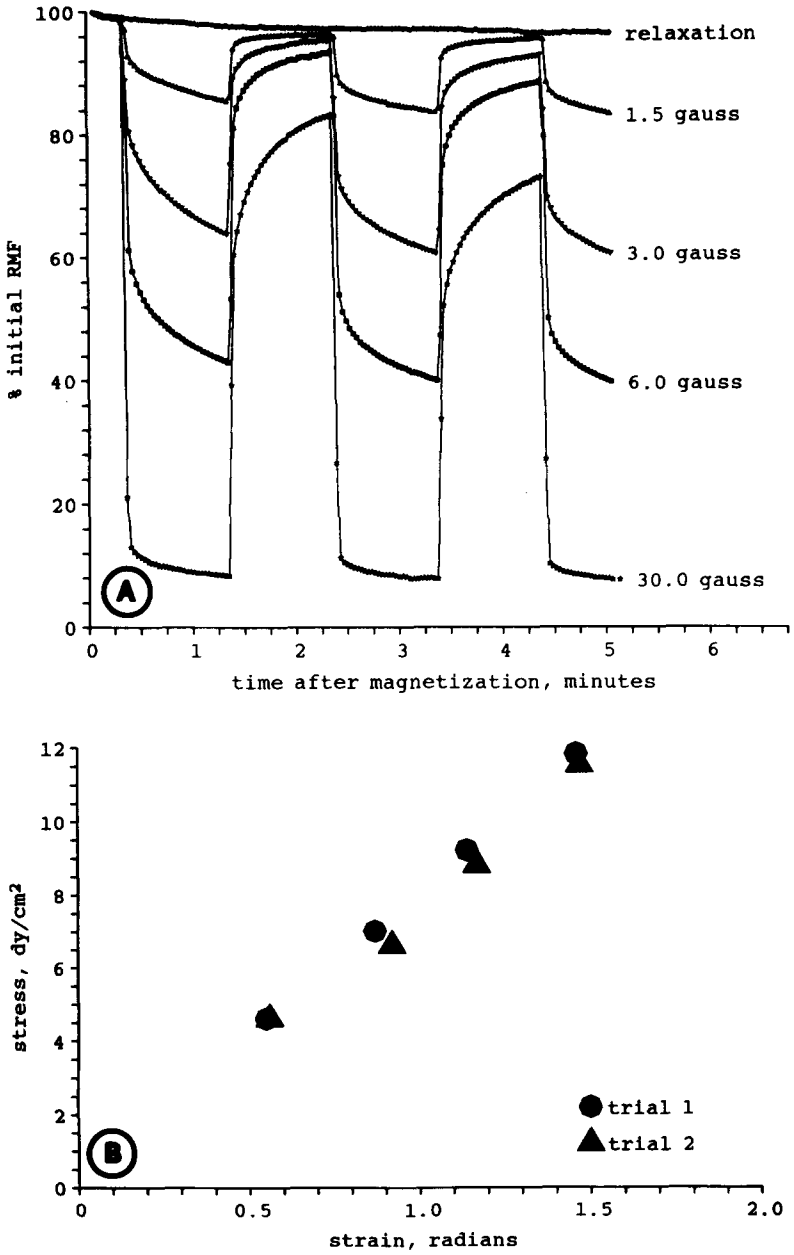

Figure 5. (*A*) The RMF shows progressively larger decrements (strain) as the magnitude of the stress (the twisting field) was varied over 1.5, 3, 6, and 30 gauss. (*B*) Plot of the stress-to-strain ratio which is derived from data such as that shown in *A*. The rigidity, as reflected in the slope of this curve, is constant, suggesting that the twisting procedure is not disruptive of the actin filamentous structure.

60 s, is nearly 20-fold lower than the actin control. Thus, addition of ABP increased the apparent rigidity by a factor of ~20. For comparison, the compliance of aliquots of the actin and the actin plus ABP samples measured by the viscoelastometer is shown in Fig. 6 *B*. Similar results were obtained by the two methods for both samples, however, a larger ABP-induced decrease in compliance was indicated by the magnetic particle method. The behavior of actin plus ABP gels,

Table I. G_{60}, Stress-to-Strain Ratio at 60 s after Stress Application

	Twisting field	First trial			Second trial		
		Stress (σ)	Strain (γ)	G_{60} (σ/γ)	Stress (σ)	Strain (γ)	G_{60} (σ/γ)
	gauss	*dyne/cm²*	*radians*	*dyne/cm²*	*dyne/cm²*	*radians*	*dyne/cm²*
F-Actin*	1.5	4.6	0.55	8.4	4.6	0.56	8.2
	3.0	7.0	0.87	8.0	6.6	0.92	7.2
	6.0	9.2	1.14	8.1	8.8	1.16	7.6
	30.0	11.8	1.46	8.1	11.5	1.47	7.8
F-Actin + ABP	6.0	21.4	0.185	116	21.3	0.190	112
	30.0	90.5	0.591	153	89.3	0.609	147

* Actin concentration of 4 mg/ml.

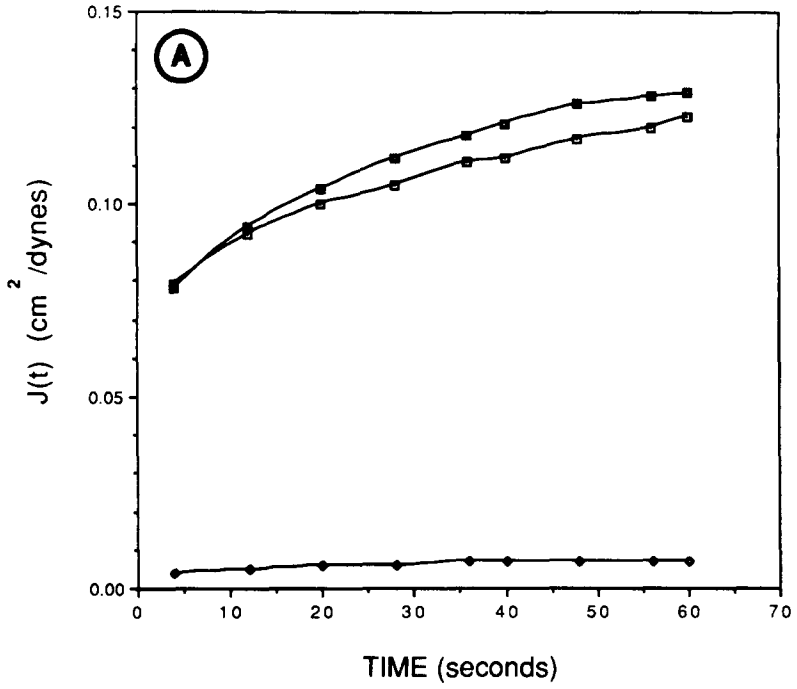

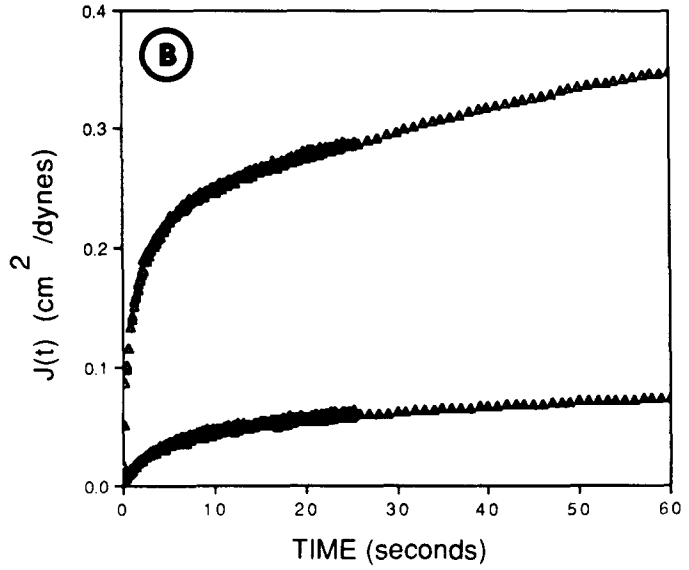

Figure 6. (*A*) The compliance, $J(t)$, as a function of time for actin and actin plus ABP mixtures calculated from curves such as are shown in Fig. 5 *A* and Fig. 7, *A* and *B*. (□) 4 mg/ml actin; (◆) 4 mg/ml actin with the ratio of actin to ABP at 200:1. (*B*) The compliance of actin and actin plus ABP mixtures as measured by the viscoelastometer. (△) 4 mg/ml actin; (▲) 4 mg/ml actin with the ratio of actin to ABP at 200:1.

as measured by magnetometry, is qualitatively in good agreement with previously reported values; the magnetic particle approach gives a compliance for actin about a factor of two lower and for actin plus ABP a factor about six lower as compared with viscoelastometry (Zaner, 1986).

Magnetometric Studies of Hamster Lung Macrophages

Fig. 8 *A* depicts both relaxation and response to twist of hamster lung macrophages. The RMF curves were generated from $\sim 10^5$ adherent cells containing a total of ~ 7 μg of γ-Fe_2O_3. The upper curve of Fig. 8 *A* shows that relaxation for particles in cell vesicles is typically quite rapid, reflecting active biochemical processes moving and rotating cell organelles (Valberg, 1984). The lower curve shows the result of applying the same twist protocol to the macrophages as was used for F-actin gels; the field used was 25 gauss. Comparing this result with Fig. 7 *A* shows that the elasticity of the cytoplasm would be better approximated by an F-actin plus ABP gel than an F-actin solution. From the RMF curve, we can calculate that, at a shear rate of 0.005/s, the apparent viscosity of the cytoplasm is 25,000 poise, in agreement with values previously reported (Valberg and Feldman, 1987).

A closer comparison of F-actin plus ABP and macrophage cytoplasm is provided in Fig. 8 *B*. These curves result from dividing the respective twist curves by their respective relaxation curves to produce a normalized curve representing the result of "twist only." The assumption made here is that relaxation and twist processes occur simultaneously but indepen-

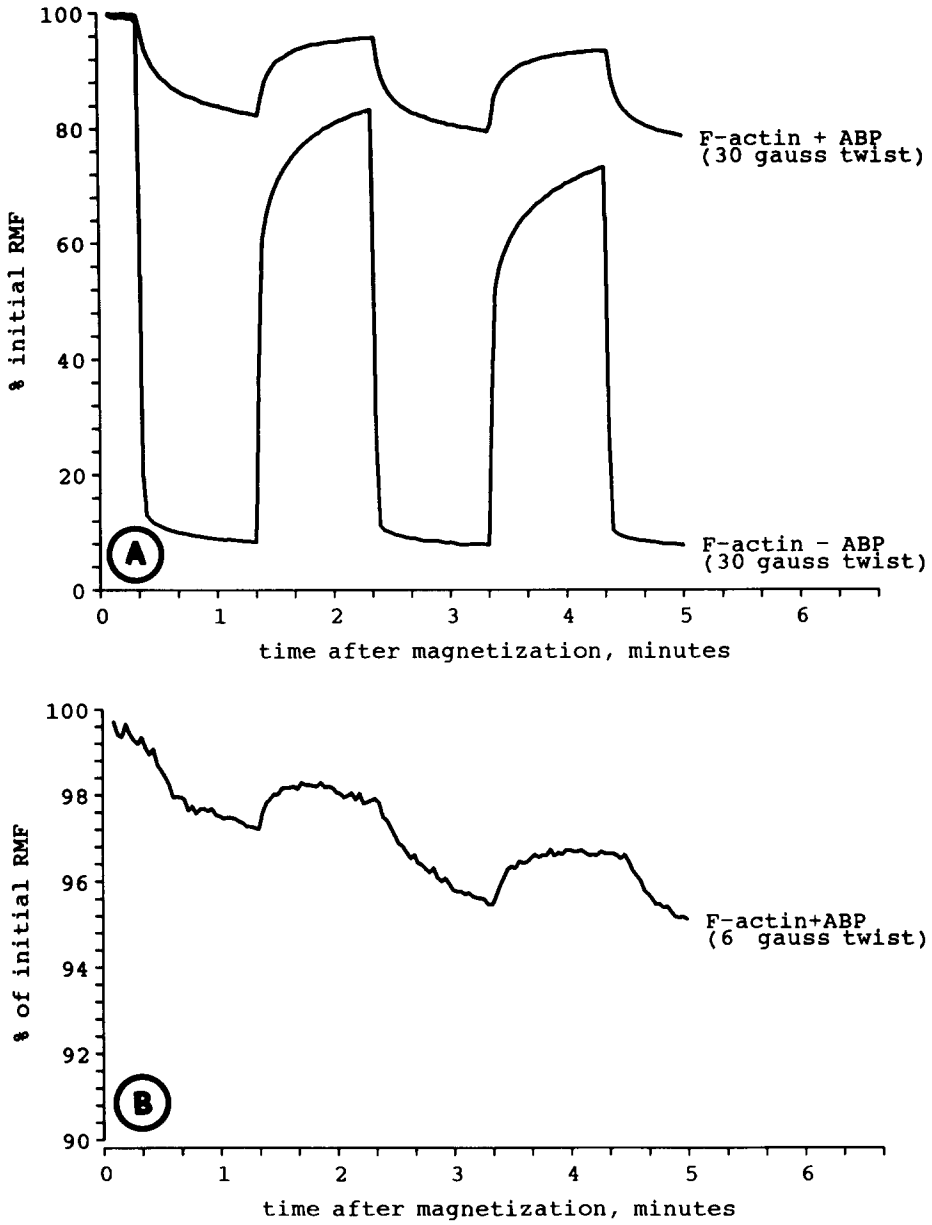

Figure 7. (*A*) The effect of adding ABP to F-actin solutions (actin-to-ABP molar ratio is 200:1). Both curves are for equivalent F-actin concentrations (4 mg/ml) and equivalent applied stress (30 gauss). (*B*) Application of a 6-gauss stress barely causes any particle twisting in an F-actin plus ABP gel. The vertical scale has been magnified ten times over *A*.

dently. That is, if the two processes are represented in the differential equation for particle motion as two separate terms summed together, then the solution to that equation of motion will consist of two functions multiplied together. This cannot be rigorously true but does provide a semiquantitative basis for comparing the two results. The curves suggest that cytoplasmic rigidity is comparable with but somewhat less than F-actin (4 mg/ml) plus ABP in a 1:200 molar ratio. Viscous losses also appear to play a greater part in cytoplasm in that consistently less of the particle orientation is recovered upon release of the twist. Finally, in cytoplasm, there appears to be a transition between a fast and a slow component to the twist and recoil responses, as indicated in two cases by the arrowheads. The fast component may represent a more compliant component of cytoskeletal organelle tethering that reaches the limit of its movement after a certain level of stress has been exceeded.

Discussion

We applied two separate techniques to equivalent F-actin samples and contrasted the results of a macroscopic linear shear technique vs. a microscopic rotational shear technique; we contrasted a single centrally located "macroscopic" source of stress vs. "dispersed" microscopic torsional stress. Interestingly, even though the techniques represent radically different approaches to probing the viscoelasticity of F-actin gels, the results were quite comparable. Thus, the magnetic movement of incorporated particles promises to be of value in elucidating the mechanical properties of purified protein systems. Moreover, the magnetic microparticle technique can be used in situations where physical or optical contact with the sample is not feasible.

Viscoelastic properties of cytoplasm play a role in the mechanisms by which living cells maintain and alter their

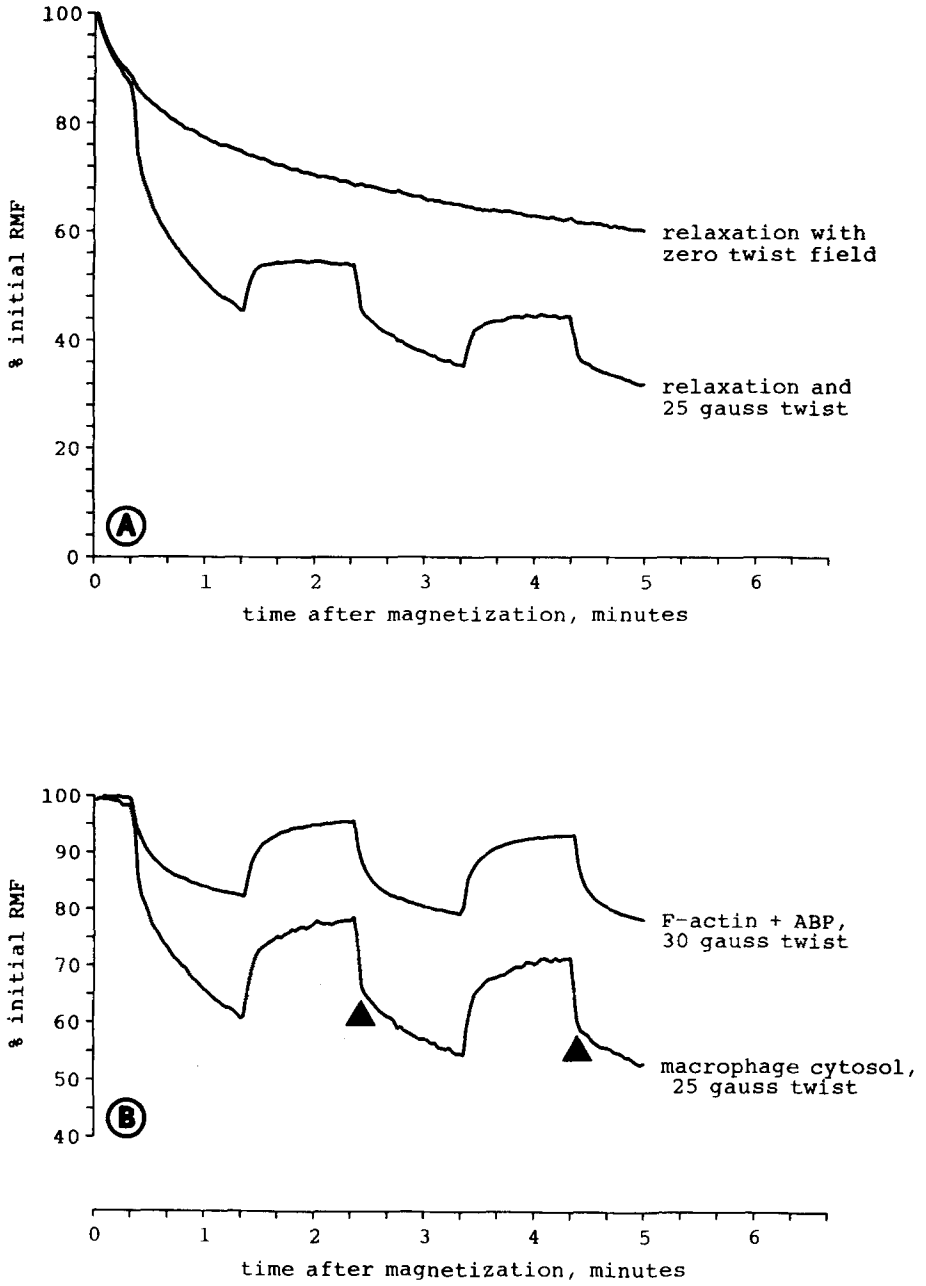

Figure 8. (*A*) RMF curves for particles within hamster lung macrophages maintained in culture at 37°C. The upper curve shows that active biochemical processes driving organelle motion cause rapid relaxation of the RMF. The lower curve shows that twisting with a field of 25 gauss causes additional decrement in the RMF, but the rate at which it occurs indicates that the interior of living cells has high apparent viscosity. (*B*) Comparison of twist responses of F-actin plus ABP and macrophage cytoplasm where the differing relaxation responses have been removed by normalization (see text).

shape. The magnetometric measurement of incorporated ferric oxide particles is one of the few methods devised to measure cytoplasmic mechanical properties. One purpose of the studies reported here was to apply the same method to obtain data from simple model protein systems that approximate the conditions present in cortical cytoplasm (Hartwig and Shevlin, 1986); this represents a step toward interpreting the viscoelasticity of living cytoplasm in molecular terms. It suggests further application of magnetic particles to assess how cytoskeletal modification (alteration of the integrity of microfilaments, microtubules, or intermediate filaments) alters the physical consistency of cytoplasm. In addition, the magnetic particle method can be applied to in vivo phenomena (i.e., for cells within the living animal).

Our F-actin data showed increasing rate of randomization of particle magnetic orientation with decreasing actin concentration. The fact that the particles undergo Brownian motion in an F-actin solution suggests that the particles are not bound to long actin filaments but, rather, are free to move through the pores between filaments. Addition of ABP does little to alter the rate of relaxation, suggesting that the predominant mechanism of relaxation is diffusion of the particles, which is considerably faster than diffusion of actin filaments.

The application of a magnetic torque to the particles causes an initial rapid twisting motion. The initial rate of rotation is much faster than that observed in viscous standards and illustrates the fact that the origin of the very high viscosities in actin solutions is a cooperative effect among filaments rather than molecular friction, as is the case for the viscosity of a homogeneous fluid. It should be noted that our results for the viscosity of actin gels and for the viscosity of cytoplasm are much higher than results obtained from the diffusion of molecules through cytoplasm (Mastro et al., 1984; Salmon

et al., 1984; Luby-Phelps et al., 1986). This difference arises because our particles are typically the size of cell organelles – i.e., much larger than molecules. As Luby-Phelps and colleagues reported, the "open spaces" in cytoplasm are likely <40 nm, and within them solvent viscosity is only about four times that of water (Luby-Phelps et al., 1986).

F-actin solutions have a significant elastic component, as evidenced by a significant recovery of particle orientation when the magnetic torque is removed. Loss of strain recovery after the first twist cycle may be due to randomization of a small fraction of magnetic particles not large enough to be effectively trapped in the F-actin matrix. The amount of recovered strain decreases for subsequent on and off cycles, which can represent either an alignment of the filaments that cannot relax within the time frame of the measurement or disruption of some actin filament structure. The latter explanation seems less likely than the former since a second series of torques demonstrates the same behavior. Moreover, actin filament solutions, which can be considered as viscoelastic solids on one time scale, may behave as (dissipative) fluids on longer time scales.

The incorporation of ABP into the actin solutions increases the resistance to twist of the particles by more than 20-fold. In addition, there is complete recovery after removal of the magnetic torque. The very high resistance to particle rotation most likely represents the fact that when the filaments are physically cross-linked into a network, movement of the particles cannot occur by rotation of the filaments, but requires bending of the filaments near the cross-link point.

The methods that have been previously used for determining the mechanical properties of F-actin systems have been essentially bulk measurements. The sample is placed between two surfaces, and the displacement or strain of the sample is observed in response to an applied force or stress. The validity of the measurement is based on the assumption that the sample is continuous and homogeneous in the region between the surfaces and that shear occurs uniformly across the sample. In contrast, the magnetic particle method produces a measurement that reflects the local environment of the particle and therefore is a kind of microscopic rheology which should be less affected by long-range heterogeneity or domain-like structure. Magnetic particle results are therefore complementary to more conventional measurements.

It is interesting to consider why the two methods yield quantitatively different results. Recent data suggest that the actin concentration is not completely uniform across a sample but, rather, varies in density within the sample (Cortese and Frieden, 1988) and may undergo phase separation into regions of higher and lower actin concentration (Newman et al, 1989). The fact that the rigidity of the actin sample is higher by the magnetic particle technique than with a conventional technique implies that the domain of high concentration is large in comparison with the size of the magnetic particles. Although our samples were sonicated to disperse the magnetic particles (subsequent to addition of salt, but before measurement), inhomogeneity in actin concentration may be the result of actin polymerizing in the "shear field" induced by stirring. Our data cannot distinguish between this mechanism and any tendency of undisturbed actin to partition itself into regions of different concentration. Further, the larger discrepancy observed in the presence of ABP implies that the cross-linking increases the heterogeneity of the sample. A possible explanation here is that the ratio of ABP to actin may fix the local concentration of protein. This interpretation is consistent with the increase in the effect of ABP at a fixed ratio to actin, as the protein concentration increases (Zaner, 1986). One can envision domains of ABP-cross-linked actin networks that progressively coalesce at increasing total protein concentration.

We conclude that the magnetic particles are useful for probing the physical properties of continuous gels as well as of living cytoplasm. The particles can be suspended in gels or can be phagocytized by cells into intracytoplasmic vesicles. Orientation and realignment can be carried out nonoptically in vivo and in vitro. From the RMF curves, diffusion mobility, rigidity, and viscosity can be extracted.

This study was supported by grants CA-40696, GM-37590, HL-31029, and HL-36427 from the National Institutes of Health.

Received for publication 31 January 1989 and in revised form 5 July 1989.

References

Buxbaum, R. E., T. Dennerll, S. Weiss, and S. R. Heidemann. 1987. F-Actin and microtubule suspensions as indetermediate fluids. *Science (Wash. DC).* 235:1511-1514.

Cortese, J. D., and C. Frieden. 1988. Microheterogeneity of actin gels formed under controlled linear shear. *J. Cell Biol.* 107:1477-1487.

Elson, L. E. 1988. Cellular mechanics as an indicator of cytoskeletal structure and function. *Annu. Rev. Biophys. Biophys. Chem.* 17:397-430.

Hartwig, J. H., and P. Shevlin. 1986. The architecture of actin filaments and the ultrastructural location of actin-binding protein in the periphery of lung macrophages. *J. Cell Biol.* 103:1007-1020.

Hartwig, J. H., and T. P. Stossel. 1981. The structure of actin-binding protein molecules in solution and interacting with actin filaments. *J. Mol. Biol.* 145:563-581.

Luby-Phelps, K., L. D. Taylor, and F. Lanni. 1986. Probing the structure of cytoplasm. *J. Cell Biol.* 102:2015-2022.

Mastro, A. M., M. A. Babich, W. D. Taylor, and A. D. Keith. 1984. Diffusion of a small molecule in the cytoplasm of mammalian cells. *Proc. Natl. Acad. Sci. USA.* 81:3414-3418.

Nemoto, I. 1982. A model of magnetization and relaxation of ferrimagnetic particles in the lungs. *IEEE (Inst. Electr. Electron. Eng.) Trans. Biomed. Eng.* 29:745-752.

Nemoto, I., K. Ogura, and H. Toyotama. 1989. Estimation of the energy of cytoplasmic movements by magnetometry: effects of temperature and intracellular concentration of ATP. *IEEE (Inst. Electr. Electron. Eng.) Trans. Biomed. Eng.* 36:598-607.

Newman, J., N. Mroczka, and K. L. Schick. 1989. Dynamic light scattering measurements of the diffusion of probes in filamentous actin subunits. *Biopolymers.* 28:655-666.

Salmon, E. D., W. M. Saxton, R. J. Leslie, M. L. Karow, and J. R. McIntosh. 1984. Diffusion coefficient of fluorescein-labeled tubulin in the cytoplasm of embryonic cells of sea urchin: video image analysis of fluorescence redistribution after photobleaching. *J. Cell Biol.* 99:2157-2164.

Sato, M., G. Leimback, W. H. Schwarz, and T. D. Pollard. 1985. Mechanical properties of actin. *J. Biol. Chem.* 260:8585-8592.

Spudich, J. A., and S. Watt. 1971. The regulation of rabbit skeletal muscle contraction. *J. Biol. Chem.* 246:4866-4871.

Stossel, T. P. 1988. The mechanical properties of white blood cells. *In* Inflammation: Basic Principles and Clinical Correlates. J. I. Gallin, I. M. Goldstein, and R. Snyderman, editors. Raven Press, New York. 325-342.

Valberg, P. A. 1984. Magnetometry of ingested particles in pulmonary macrophages. *Science (Wash. DC).* 244:513-516.

Valberg P. A., and D. F. Albertini. 1985. Cytoplasmic motions, rheology, and structure probed by a novel magnetic particle method. *J. Cell Biol.* 101: 130-140.

Valberg, P. A., and J. D. Brain. 1979. Generation and use of three types of iron-oxide aerosol. *Am. Rev. Respir. Dis.* 120:1013-1024.

Valberg, P. A., and J. P. Butler. 1987. Magnetic particle motions within living cells: physical theory and techniques. *Biophys. J.* 52:537-550.

Valberg, P. A., and H. A. Feldman. 1987. Magnetic particle motions within living cells: measurement of cytoplasmic viscosity and motile activity. *Biophys. J.* 52:551-561.

Zaner, K. S. 1986. The effect of the 540-kilodalton actin cross-linking protein, actin binding protein, on the mechanical properties of F-actin. *J. Biol. Chem.* 261:7615-7620.

Zaner, K. S., and J. H. Hartwig. 1988. The effect of filament shortening on the mechanical properties of gel-filtered actin. *J. Biol. Chem.* 263:4532-4536.

Zaner, K. S., and T. P. Stossel. 1983. Physical basis of the rheologic properties of F-actin. *J. Biol. Chem.* 258:11004-11009.

Zaner, K. S., R. Fotland, and T. P. Stossel. 1981. Low-shear, small-volume viscoelastometer. *Rev. Sci. Instrum.* 52:85-87.